

ARTICLE TYPE

Relativistic X-ray jets at high redshift

Daniel A Schwartz^{*1} | Aneta Siemiginowska¹ | Diana M Worrall² | Mark Birkinshaw² | Teddy Cheung³ | Herman Marshall⁴ | Guilia Migliori⁵ | John Wardle⁶ | Doug Gobeille⁷

¹High Energy Astrophysics, Smithsonian Astrophysical Observatory, Massachusetts, USA

²HH Wills Physics Laboratory, University of Bristol, UK

³Space Science Division, Naval Research Laboratory, Washington D C, USA

⁴Kavli Institute, MIT, Massachusetts, USA

⁵INAF Istituto di Radioastronomia, Italy

⁶Physics Department, Brandeis University, Massachusetts, USA

⁷Physics Department, University of Rhode Island, Rhode Island, USA

Correspondence

^{*}60 Garden St., Cambridge, MA 02138, USA. Email: dschwartz@cfa.harvard.edu

Powerful radio sources and quasars emit relativistic jets of plasma and magnetic fields that travel hundreds of kilo-parsecs, ultimately depositing energy into the intra- or inter-cluster medium. In the rest frame of the jet, the energy density of the cosmic microwave background is enhanced by the bulk Lorentz factor as Γ^2 , and when this exceeds the magnetic energy density the primary loss mechanism of the relativistic electrons is via inverse Compton scattering. The microwave energy density is also enhanced by a factor $(1+z)^4$, which becomes important at large redshifts. We are using *Chandra* to survey a $z>3$ sub-sample of radio sources selected with 21 cm-wavelength flux density > 70 mJy, and with a spectroscopic redshift. Out of the first 12 objects observed, there are two clear cases of the X-rays extending beyond the detectable radio jet.

KEYWORDS:

galaxies: jets – radiation mechanism: non-thermal – radio continuum: galaxies – quasars: general – X-rays: galaxies

1 | INTRODUCTION

The number of quasars known in the redshift range $z>3$ and beyond $z=6$ has exploded in recent years, with the Sloan Digital Sky Survey (SDSS) playing a key role. At redshift 7 the Universe is less than a billion years old, and at redshift 3 only about 2 billion years, or 15% of the current age estimate based on the Planck satellite measurements (Planck Collaboration, Aghanim, Akrami, & Ashdown, 2017) of the cosmic microwave background (CMB)¹. Following these results, we expect the facilities coming on line in the next decade, such as SKA, the LSST, JWST, and the proposed *Lynx* X-ray observatory, to allow us to trace formation and growth from the first massive black holes and galaxies to the present cosmic epoch. X-ray observations will play a crucial role in delineating this development of structure in the Universe. The proposed *Lynx* observatory (<https://arxiv.org/abs/1809.09642>), with an effective area of 2 m² and angular resolution of 0'5 will have the

capability to detect black holes of only $10^4 M_\odot$ at redshift $z=10$ in the deepest surveys. However, even prior to *Lynx*, all-sky X-ray surveys, and high resolution observations with *Chandra*, may reveal previously unknown active galaxies at redshifts $z>5$ via their X-ray jet emission (Schwartz, 2002).

A *Chandra* survey of radio quasars with arcsec scale radio jets detected about 2/3 of the targets in short, 5 to 10 ks, observations (Marshall et al., 2018). The redshifts of those quasars ranged from 0.1 to 2.1. The X-ray emission is interpreted most simply as radiation from inverse Compton up-scattering of the cosmic microwave background photons (IC/CMB) within a kpc-scale jet that is moving relativistically (bulk Lorentz factor $\Gamma \geq 3$) with respect to the co-moving frame of the parent quasar. The bulk relativistic motion explains the one-sided nature of the jets via Doppler boosting, and is indicated by apparent superluminal motion and by radio brightness temperatures in excess of 10^{12} K on pc and sub-pc scales. In the presence of magnetic fields and photons, relativistic electrons will scatter off both, emitting synchrotron radiation and IC radiation. The dominant energy loss for the electrons simply depends on the energy density of the target fields or photons.

¹In this article we will use the parameters $H_0=67.3$ km s⁻¹ Mpc⁻¹, $\Omega_m=0.315$, and $\Omega=1$ from those Planck results

The Compton scattering is often called “external Compton” to distinguish from synchrotron self-Compton emission. In the rest frame of a relativistic jet, the external photons will appear highly anisotropic, and their energy density appear enhanced by a factor approximately Γ^2 . The scattered radiation is highly anisotropic in the frame of an observer that is nearly at rest with respect to the CMB. The intensity is enhanced, or diminished, by a factor $\delta^{3+\alpha}$ where $\delta = 1/(\Gamma(1 - \beta \cos[\theta]))$ is the Doppler factor. Here α is the spectral index of the radiation (defined for flux density $\propto \nu^{-\alpha}$), $\Gamma = 1/\sqrt{1 - \beta^2}$ is the bulk Lorentz factor of the jet and θ is the angle from the jet direction to the observer line of sight.

At lower redshifts the IC/CMB mechanism is not usually dominant. X-rays from FR I type radio jets are best explained as an extension of the radio synchrotron spectrum (Harris & Krawczynski, 2006). For several quasars the gamma-rays which are predicted by IC/CMB fall above upper limits from the Fermi gamma-ray telescope (Breiding et al., 2017). However, since the energy density of the CMB increases with redshift as $(1+z)^4$, IC/CMB eventually becomes dominant. Figure 1 plots the magnetic field strength vs. redshift at which magnetic and CMB energy densities become equal. This occurs at redshifts (Schwartz, 2002)

$$z \geq \max[(0.556\sqrt{B_{\mu G}/\Gamma} - 1), 0]. \quad (1)$$

The figure shows four cases, $\Gamma = 1, 4, 9$, and 16 . For magnetic field strengths below the curve for the given value of Γ , IC/CMB will dominate. At redshifts greater than 3 this occurs for magnetic fields weaker than $50 \mu\text{Gauss}$, even for bulk motion with $\Gamma \approx 1$, and occurs for fields weaker than 100 's of μGauss for modest values of Γ . For comparison, magnetic fields in lower redshift jets are typically estimated to be a few 10 's of μGauss .

Very near a quasar, photons from the accretion disk, the broad line clouds, and the dusty torus will dominate. The IC/CMB will be the dominant external Compton mechanism at distances from the quasar core

$$r_{kpc} \geq 14.13\sqrt{L}/(\Gamma(1+z)^2), \quad (2)$$

where L is the radiative luminosity of the quasar in units of $10^{44} \text{ erg s}^{-1}$.

Jets at high redshift should increasingly manifest as X-ray jets rather than radio jets. Two factors favor the X-ray emission. The first results from the cosmological diminution of surface brightness, which is proportional to $(1+z)^{-4}$. This reduces the ability to detect extended radio sources. However, for IC/CMB X-ray emission this is compensated by the $(1+z)^4$ increase of the CMB energy density. The second factor is due to the shorter lifetimes of the electrons emitting GHz synchrotron radiation. Very roughly, electrons with Lorentz factor $1000/\Gamma$ are producing the 1 keV radiation. Figure 2 shows the lifetime for such

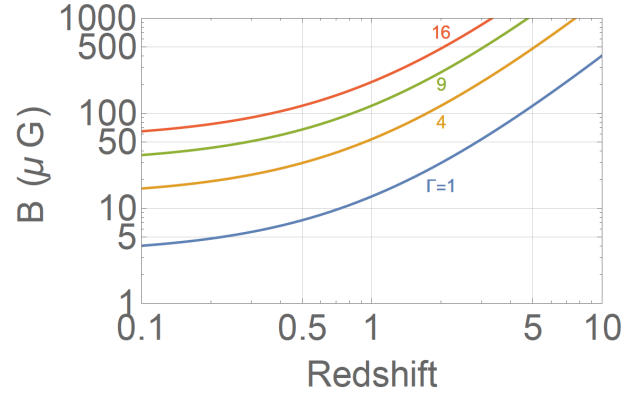


FIGURE 1 Criteria for IC/CMB radiation to dominate electron energy loss. The line for each value of Γ plots the magnetic field strength for which the magnetic energy density equals the CMB energy density as a function of redshift. For a jet at a given redshift, the IC/CMB mechanism will dominate unless the magnetic field is stronger than that given on the curve of the appropriate Lorentz factor Γ .

electrons to lose energy via IC/CMB as a function of redshift and of the jet bulk Lorentz factor. GHz synchrotron radiation in a $10 \mu\text{Gauss}$ field is produced by electrons with $\gamma \approx 10^4$. Such electrons will up-scatter the CMB to energies of 100Γ keV, while also emitting GHz synchrotron radiation. So at redshift 3, for a typical Γ of 10, the X-ray jet lifetime is 100 times longer than the GHz radio jet.

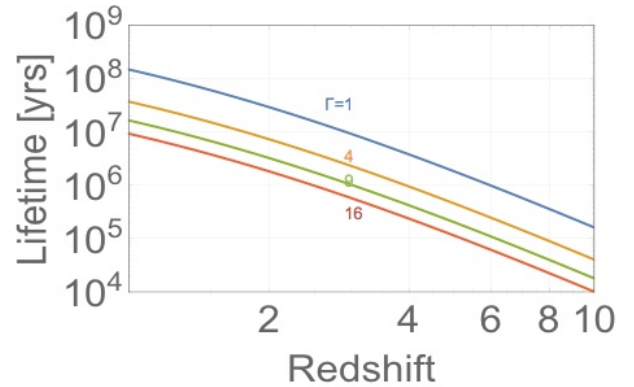


FIGURE 2 Lifetime of electrons emitting approximately 1 keV X-rays via the IC/CMB mechanism. From top to bottom, the curves give the lifetime for X-ray jets with bulk Lorentz factors $\Gamma = 1, 4, 9$, and 16 , respectively. Losses due to synchrotron radiation are assumed to be much less than to IC/CMB.

The radio source J0730+4049 at $z=2.50$, (B3 0727+409), was discovered with a $12''$ long X-ray jet with no extended radio emission except for one knot $1''.4$ along the X-ray jet from the quasar core (Simionescu et al., 2016). Based on that discovery, and the rationale discussed above, we have undertaken a *Chandra* survey for more systems dominated by X-ray jets.

2 | THE HIGH REDSHIFT SURVEY

Our sample is based on a survey conducted by Gobeille, Wardle, & Cheung (2014). That survey covered the area jointly observed in the FIRST radio survey (Becker, White, & Helfand, 1995) and optically by the Sloan Digital Sky Survey (SDSS). It contains all 123 quasars at redshifts ≥ 2.5 with a spectroscopic redshift measured in the SDSS, and with a radio flux density greater than 70 mJy at 1.4 GHz (Gregory, Scott, Douglas, & Condon, 1996). The radio flux was summed from the total system, including any extended emission. Of the quasars, 61 showed extended emission. Thirty of these were classified as triples, and as such we considered that they were probably not beamed in our direction. Of the remaining 31, we selected the 16 with redshift $z > 3$ as most likely to be detectable IC/CMB radiators in 10 ks *Chandra* observations. The two at the largest redshifts, J1430+4204 at $z=4.7$ and J1510+5702 at $z=4.3$, had previously been detected at 1.9 counts ks^{-1} (Cheung et al., 2012) and 1.4 counts ks^{-1} (Siemiginowska et al., 2003), respectively, and were not re-observed.

3 | DETECTION OF X-RAY JETS

Table 1 shows the sample of 14 objects, plus the two previously detected. The 14 were accepted as 10 ks *Chandra* observations in cycle 19. The first two columns give an abbreviated source name, and the redshift. In column 3 we predicted the counts expected in the 0.5–7 keV band if their flux scaled from that of J1430+4204 and J1510+5702 simply by the ratio of $(1+z)^4$ for their redshifts. The counting rates of those two sources previously detected do have a ratio very nearly $(5.72/5.30)^4$. We expected this number to be a conservative mean, with some jets much brighter than predicted. The last column indicates whether an X-ray jet was detected. For J1405 and J1610 we do have statistically significant detections, with the number of counts as tabulated. For 10 other quasars, we do not have significant indication of a jet.

For the systems without an apparent jet, the exact upper limit must be carefully considered for each case. To get a rough idea, since we typically can expect one scattered X-ray from the quasar core, and negligible background in 10 ks, four counts would be a detection to 98% confidence for any one source. However, since we have 14 targets, we require 5 counts such

TABLE 1 *Chandra* High Redshift Sample: $z > 3$

Source Name	Redshift	Predicted Counts per 10 ks	Detected Jet Counts?
J1435+5435	3.809	9.5	NO
J0833+0959	3.731	8.9	?
J1223+5038	3.501	7.3	NO
J0933+2845	3.421	6.8	NO
J0909+0354	3.288	6.0	NO
J0801+4725	3.267	5.9	NO
J1655+1948	3.26	5.8	NO
J1616+0459	3.215	5.6	NO
J1405+0415	3.209	5.6	YES, 7
J1655+3242	3.189	5.5	NO
J1610+1811	3.118	5.1	YES, 8
J1016+2037	3.115	5.1	NO
J1128+2326	3.049	4.8	?
J0805+6144	3.033	4.7	NO
J1430+4204	4.72	19	YES
J1510+5702	4.30	14	YES

J0833+0959 and J1128+2326 have not yet been observed.

that none of the 14 would give a spurious detection to 98% confidence.

When we do detect $N < 5$ counts, then we must ask how many counts might have been expected such that to 98% confidence only N resulted from our observation. If N is 4, the upper limit would be 10.6. That calculation assumes that we have one specific area to search, e.g., along the direction of a radio jet, knot, or lobe. In view of these statistical complications, we must perform further analysis for the sources which are not detected, and only enter a “NO” in Table 1. We present preliminary results on the two detections.

3.1 | J1405+0415

Figure 3 shows the 0.5 to 7 keV X-ray data from our observation of J1405+0415. We have superposed contours from our JVLA observations centered at 6.2 GHz. The X-ray jet is seen as an extension along the line at position angle 231° from the quasar core through the radio knot $0''.8$ away. There is no radio emission detected along this line past $0''.8$. The knot has a flux density 28 mJy and a radio spectral index $\alpha = 0.91 \pm 0.09$. At position angle 255° there is a very faint radio lobe $3''.3$ from the core, with flux density 2.9 mJy and spectral index 1.66 ± 0.4 .

In the core, Yang, Gurvits, Lobanov, Frey, & Hong (2008) measure many components with VLBI and VSOP data. The 4.86 GHz VSOP data show a range of position angles from

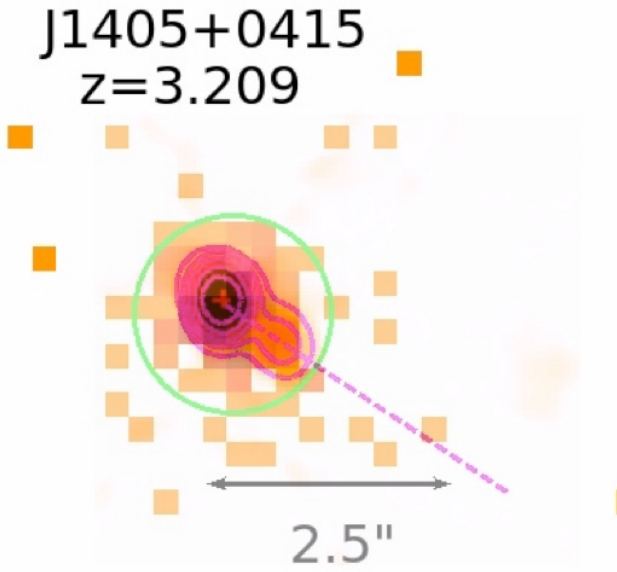


FIGURE 3 Contours of the 6.2 GHz radio emission, superposed on the pixelated X-ray counts. Radio contours (magenta in the on-line version) start at 3.3 mJy/beam and are logarithmically spaced to the peak of 694 mJy/beam. Restoring beam is $0''.39 \times 0''.32$. X-ray pixels are $0''.24$ square. Quasar peak is 31 counts per pixel. Outside the 1 arcsec radius circle centered on the quasar (green in the on-line version) the pixels have at most one count. The dashed line extension from the quasar through the radio knot suggests the direction of a jet, and 7 X-ray photons are found along this line where only 0.9 are expected from background and from scattered quasar photons.

282° to 335° at distances $0''.5$ to $13''.2$ from the core, and with sizes $0''.3$ to $2''.5$. From several components in the core which show brightness temperatures in excess of 10^{12} K they conclude there is relativistic motion.

The jet X-ray flux is 9×10^{-15} erg cm $^{-2}$ s $^{-1}$, which would correspond to a luminosity of 8×10^{44} erg s $^{-1}$ if it were isotropically emitted. The quasar core has 269 photons, giving an X-ray flux of 3.3×10^{-13} erg cm $^{-2}$ s $^{-1}$ and a luminosity of 3.2×10^{46} erg s $^{-1}$. Thus the jet X-ray flux is 2.6% that of the quasar core, with a factor of 2 uncertainty.

3.2 | J1610+1811

Figure 4 plots the 0.5 to 7 keV X-ray data from our observation of J1610+1811. There is significant X-ray emission along the dashed line that extends from the quasar radio core to an extended radio lobe. The 8 counts associated with the jet correspond to a flux of 10^{-14} erg cm $^{-2}$ s $^{-1}$. If interpreted as isotropic emission, the luminosity would be 9×10^{44} erg s $^{-1}$. Those numbers could be a factor of 2 larger or smaller due to the detection

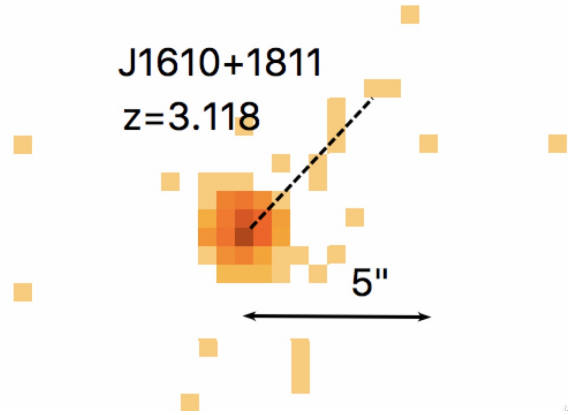


FIGURE 4 The 0.5–7 keV X-ray counts are binned in $0''.49$ pixels. The quasar peak has 104 counts. More than 2 pixels (1 arcsec) from the core, pixels have at most one count. The dashed line at position angle 316.5° is on the line from the quasar to an extended radio lobe $4''.8$ away. The eight X-ray counts which are along this line constitute a significant detection of a jet. No radio emission is detected between the quasar and the lobe in our JVLA observations centered at 6.2 GHz.

being just above threshold. The quasar core has 331 X-ray counts. This is a measured flux of 5.2×10^{-13} erg cm $^{-2}$ s $^{-1}$ or an isotropic luminosity of 4.6×10^{46} erg s $^{-1}$. The X-ray jet flux is apparently 2% (between 1% and 4% to 95% confidence) of the quasar X-ray flux.

A 2 mas long jet extends in the same direction in an 8.4 GHz VLBI observation by Bourda, Collioud, Charlot, Porcas, & Garrington (2011). Our JVLA observations centered at 6.2 GHz show no indication of emission outside of the $0''.5$ region around the quasar, up to the edge of the lobe at $4''.4$ from the core, with a 1 mJy upper limit. At 6.2 GHz the flux density is 65 mJy from the core, and 8.2 mJy from the NW lobe.

The radio lobe and the VLBI structure each show a one-sided system, which indicates a relativistic jet. We can construct an illustrative IC/CMB model by taking the radio flux density to equal 1 mJy at 6.2 GHz. We use usual assumptions, (cf. Schwartz et al. (2006); Worrall & Birkinshaw (2006)) of minimum energy in the magnetic field and relativistic particles, relativistic electrons with a power law spectral index 2.1 from $\gamma=30$ to $\gamma=10^6$, a jet width of 2 kpc, charge balance provided by equal numbers of protons, and uniformly tangled and isotropic distribution of particles and fields in the jet rest frame. We make the assumption that the bulk Lorentz factor equals the Doppler factor. This is equivalent to assuming the jet is at the largest possible angle to the line of sight for the given Doppler factor. We find $\delta=\Gamma=9.4$, a magnetic field strength 12 μ Gauss, and a kinetic power 1.4×10^{46} erg s $^{-1}$. Such a jet would be at an angle 6.2° to our line of sight.

Electrons emitting the 6.2 GHz radiation have Lorentz factors $\gamma \approx 11,000$. Their lifetime against energy loss by IC scattering of the CMB is only 8500 years, compared to 880,000 years for the electrons with $\gamma \approx 100$ which are emitting 1 keV X-rays. The short radio lifetime shows that it is reasonable that only the X-rays are detectable.

With the true radio flux density being less than 1 mJy, both the magnetic field strength and the relativistic particle density will be smaller if we preserve the minimum energy assumption. In that case the jet must have a larger bulk Lorentz factor since the CMB energy density in the jet must be enhanced further in order to produce the same X-ray emission. Conversely, if the X-ray flux is at the lower limit allowed, the magnetic field strength and particle densities would be larger, and the jet Lorentz factor smaller.

4 | DISCUSSION

The numbers of predicted counts, column 3 in Table 1, assumes that the jets are identical in their intrinsic properties, magnetic field, particle density and spectrum, bulk Lorentz factor, age and size, and furthermore at the same angle to our line of sight as the object J1430+4204 from which they are scaled. This is clearly unrealistic, but does correctly predict for at least 4 of the 16 sources at redshift greater than 3, and has resulted in discovery of two new X-ray jets among the 12 quasars observed so far. For each individual source in Table 1 the upper limit may allow that the predicted counts are correct. However, the ensemble of 14 sources predicts 87 counts, where we have no more than ≈ 40 , so that clearly the average emission is less than our scaling model.

Strictly speaking, we cannot claim that we have discovered “jets” according to a common definition (Bridle & Perley, 1984) requiring the length to be at least four times the width for a radio jet. We do have definite statistical detection of X-ray emission extended outside the quasar X-ray/radio core. The emission is statistically connected to a direction defined *a priori* by radio observations, i.e., extremely unlikely to be a background or foreground source not associated with the system. However, we have no information on the structure of the X-ray jet, e.g., whether it is continuous or even just a single knot of emission.

Simionescu et al. (2016) made the critical discovery of an X-ray jet from the quasar J0730+4049, that was not coincident with a radio jet. We have now discovered two more cases of X-ray jets which are not coincident with underlying radio jets, establishing that such a class of object exists. Table 2 compares the observed properties of these three objects. The flux is taken in the 0.5 to 7 keV band. We convert to surface brightness in units of $10^{-14} \text{ erg cm}^{-2} \text{ s}^{-1} \text{ arcsec}^{-2}$ by dividing by

TABLE 2 Comparison of the X-ray dominated jets.

	J0730[†]	J1405	J1610
Redshift	2.50	3.209	3.118
Live time (ks)	19.	9.6	9.1
Counts	38	7	8
Flux $10^{-14} \text{ erg cm}^{-2} \text{ s}^{-1}$	2.7	0.9	1.
Length (arcsec)	12	3.5	4.6
Surface brightness	0.9	1.	0.9

[†]J0730 live time, counts, and length from Simionescu et al. (2016)

the tabulated length of each jet, and by an assumed $0''.25$ width for each jet. That width is roughly 2 kpc at redshifts of a few. The resulting surface brightness is remarkably similar for the three sources, but with up to a factor of two uncertainty for the two new jets reported here. This could indicate similar physical conditions in the three jets, or could just reflect that they are all near the threshold of detection for a 10 ks observation. However, a very significant difference is that the jet in J0730 is detected with an X-ray flux 23% that of the quasar, while the two new jets here have only about 2% of the quasar flux, consistent with the observations from the survey at lower redshift (Marshall et al., 2018).

These objects are potentially extremely important, because they can be detected in X-rays at whatever large redshift they exist, due to their approximately constant surface brightness. However, discovery of relativistic X-ray jets is difficult, because only the few percent of radio quasars which are beamed in our direction are candidate systems, so that it is expensive in observing time to use pointed *Chandra* observations for this purpose. We look forward to the all sky survey by the eROSITA instrument on the Spectrum X-Gamma satellite (Predehl, 2011) to provide target systems. While eROSITA does not have the angular resolution to resolve jets, it should result in unidentified blank sky sources which are candidates to be very distant “orphan” X-ray jets. These candidates will be reasonable targets for *Chandra* observations, and for the much more powerful *Lynx* observatory which is proposed to be the *Chandra* successor, with 30 times the effective area and similar angular resolution in the 0.1 to 10 keV region. Furthermore, *Lynx* will have 800 times larger grasp than *Chandra* and can therefore do surveys of tens of square degrees with similar sensitivity.

ACKNOWLEDGMENTS

This research was funded by NASA grant GO8-19077X (*Chandra*) and by NASA contract NAS8-03060 to the Chandra X-ray Center.

REFERENCES

- Becker, R. H., White, R. L., & Helfand, D. J. 1995, *ApJ*, 450, 559.
- Bourda, G., Collioud, A., Charlot, P., Porcas, R., & Garrington, S. 2011, *A&A*, 526, A102.
- Breiding, P., Meyer, E. T., Georganopoulos, M., Keenan, M. E., DeNigris, N. S., & Hewitt, J. 2017, *ApJ*, 849, 95.
- Bridle, A. H., & Perley, R. A. 1984, *ARA&A*, 22, 319-358.
- Cheung, C. C., Stawarz, Ł., Siemiginowska, A., Gobeille, D., Wardle, J. F. C., Harris, D. E., & Schwartz, D. A. 2012, *ApJ*, 756, L20.
- Gobeille, D. B., Wardle, J. F. C., & Cheung, C. C. 2014, *ArXiv e-prints*, <https://arxiv.org/abs/1406.4797>.
- Gregory, P. C., Scott, W. K., Douglas, K., & Condon, J. J. 1996, *ApJS*, 103, 427.
- Harris, D. E., & Krawczynski, H. 2006, *ARA&A*, 44, 463-506.
- Marshall, H. L., Gelbord, J. M., Worrall, D. M. et al. 2018, *ApJ*, 856, 66.
- Planck Collaboration, Aghanim, N., Akrami, Y., & Ashdown, M. e. a. 2017, *A&A*, 607, A95.
- Predehl, P. 2011, eROSITA - A new X-ray All-sky Survey. J.-U. Ness & M. Ehle (Eds.), The X-ray Universe 2011 p. 023., <http://adsabs.harvard.edu/abs/2011xru...conf...23P>.
- Schwartz, D. A. 2002, *ApJL*, 569, L23-L26.
- Schwartz, D. A., Marshall, H. L., Lovell, J. E. J. et al. 2006, *ApJ*, 640, 592-602.
- Siemiginowska, A., Smith, R. K., Aldcroft, T. L., Schwartz, D. A., Paerels, F., & Petric, A. O. 2003, *ApJ*, 598, L15-L18.
- Simionescu, A., Stawarz, Ł., Ichinohe, Y. et al. 2016, *ApJ*, 816, L15.
- Worrall, D. M., & Birkinshaw, M. 2006, Multiwavelength Evidence of the Physical Processes in Radio Jets. D. Alloin (Ed.), Physics of Active Galactic Nuclei at all Scales Vol. 693, p. 39. doi:
- Yang, J., Gurvits, L. I., Lobanov, A. P., Frey, S., & Hong, X.-Y. 2008, *A&A*, 489, 517-524.

How cite this article: Schwartz, D. A. ET AL (2019), Relativistic X-ray jets at high redshift, *Astronomische Nachrichten*, 2019;.

How cite this article: Schwartz, D. A. ET AL (2019), Relativistic X-ray jets at high redshift, *Astronomische Nachrichten*, 2019;.